MATERIAL CHARACTERISATION AND FATIGUE DATA CORRELATION OF SHORT FIBRE COMPOSITES: EFFECTS OF THICKNESS, LOAD RATIOS AND FIBRE ORIENTATION AT ELEVATED TEMPERATURES

Francesco Emanuele Fiorini[a], Luca Michele Martulli[b], Philippe Steck[a], Andrea Bernasconi[b]

a: thyssenkrupp Presta AG, Competence Center Mechanics, Principality of Liechtenstein – francesco.fiorini@thyssenkrupp-automotive.com
b: Politecnico di Milano, Department of Mechanical Engineering, Italy

Abstract: *In design engineering of short fiber reinforced components a given material can be used for two or more parts of the same system having different wall thicknesses. The thickness, together with numerous parameters, has an impact on the cyclic behavior of short fiber reinforced thermoplastics under fatigue loading. This research analyses and compares the fiber orientation by µCT as well as the quasi-static and cyclic behavior of two sets of specimens with 1.6 and 3 mm wall thicknesses made of PA6T/6I GF50. Fatigue criteria based on cyclic mean strain rate or on cyclic creep energy density are evaluated to assess the most accurate and independent of the thickness.*

Keywords: short fiber-reinforced thermoplastic; fatigue criterion; anisotropy; load ratio; thickness.

1. Introduction

In the last years, the automotive industry has been strongly impacted by the increase of restrictive CO_2 regulations on top of the already well-established aim for best cost solutions. Lightweight design and wide application of plastic materials is thus becoming of primary importance. This design can be achieved by using lightweight materials, such as Short Fibers Reinforced Polymers (SFRPs). These composite materials are usually injection molded into complex forms. Moreover, these materials can achieve a fair strength to weight ratio. To fully adopt SFRPs into automotive parts, it is necessary to be able to predict their fatigue strength. However, many challenges occur when predicting the fatigue behavior of SFRP composites. This is due to a various number of influencing parameters, which have a direct impact on the quasi-static and cyclic response. Some of these influencing parameters are the fiber orientation [1,2,3], fatigue loading [4,5], loading frequency [6] and mean stress [7]. The cyclic creep strain rate can be a unifying criterion for fatigue test results with positive stress ratios [8-10]. A unifying criterion is relevant due to its potential to accelerate the product's development time by reducing the testing effort, leading to higher efficiency and less costs. However, none of the above-mentioned authors take the wall thickness of the specimen into consideration as one potential influencing parameter. Complex systems developed for the automotive industry often comply with a modular product architecture to be able to meet the required increasing variation diversity. This results into building up components and sub-components by different means of design, one parameter being the wall thickness. In the present research, the dependency of the fatigue response of SFRPs on the thickness is investigated.

 ©2022 Francesco et al. doi:10.5075/epfl-298799_978-2-9701614-0-0 published under CC BY-NC 4.0 license

2. Material, specimen geometry and experimental method

2.1 Material

A Polyphtalamide PA6T/6I, filled with 50% weight short glass fibers (Ultramid® Advanced T1000HG10) was investigated. To investigate the influence of the thickness in combination with the fiber orientation on the mechanical properties, dog bone samples were extracted from injection molded plaques with a dimension of 150 x 150 mm and two different thicknesses t (1.6 mm and 3 mm). The plates were manufactured with the same material and appropriate process conditions by injection molding. Injection molding induces a heterogeneous orientation of the fibers through the thickness of the plates. The resulting microstructure can be described by three layers: the skin, the shell and the core [1, 11]. In the shell, the thickest part, fibers are aligned with the injection flow. A dog bone specimen was chosen for the quasi-static and cyclic characterization. Figure 1a showcases specimen's shape and dimensions (radiuses S and L are not reported due to confidentiality restrictions).

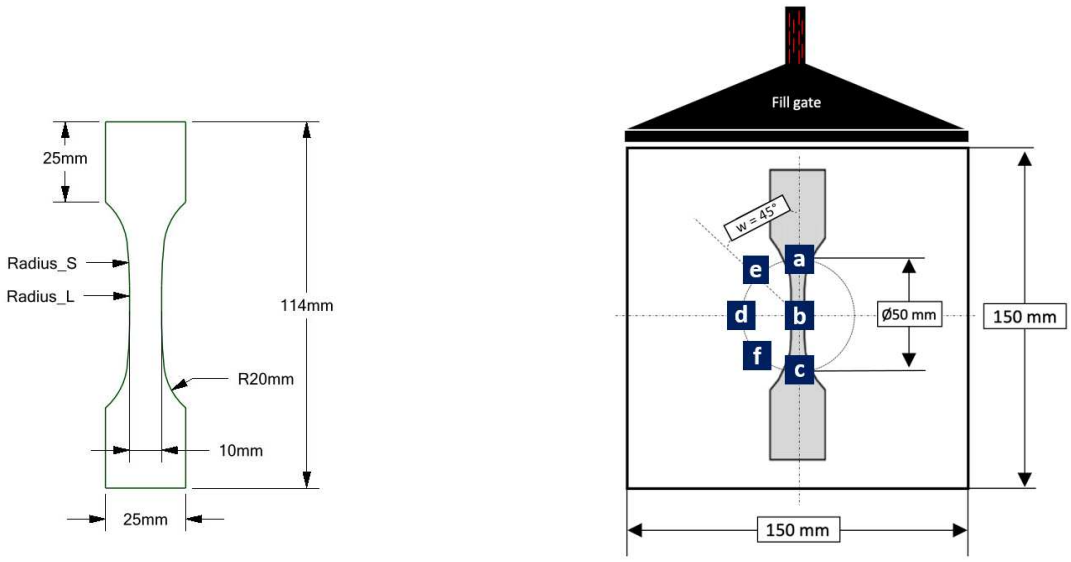

(a) *(b)*

Figure 1. Specimen dimension(a). Mold plaque dimensions and cutting sample orientation (b).

One coupon per plate was machined out by milling at 0° or 90° with respect to the main flow direction as shown in Figure 1b. The test temperature was 80°C. The relative humidity (RH) was kept under 0.1% wt., sealing the specimens in individual special bags to prevent any change in RH prior to the experiment after drying.

2.2 Methods

2.2.1 µCT Measurements

Micro Computed Tomography (µCT) samples were cut out from some of the dog bone specimens to measure the local fiber orientation. The µCT sample extraction points are shown in Figure 1b. In total, 6 positions for each plate thickness were measured. The µCT samples were 3 × 3 × t mm in size (t = 3 mm and 1.6 mm). A RX Solutions Destem 130 was used. Scanning resolution was 7 µm/voxel. Voltage acceleration and target current were 110 kV and 72 µA, respectively. Output data was processed with the software VGStudio Max by Volume Graphics.

 ©2022 Francesco et al. doi:10.5075/epfl-298799_978-2-9701614-0-0 published under CC BY-NC 4.0 license

2.2.2 Quasi-static testing

The quasi-static tests were conducted with an Inspect 300-1 Hegewald and Peschke test rig. The 3D camera optical measurement system GOM ARAMIS was used to measure the deformation of the specimens during the quasi-static experiments. A random speckle pattern was applied onto the specimens by white spray paints. To be able to carry out tests at 80°C, a temperature chamber equipped with a digital temperature controller was used. The displacement rate was 1 mm/min. Five specimens per thickness (3 mm and 1.6 mm) were tested for both orientations (0° and 90°).

2.2.3 Cyclic testing

Cyclic fatigue tests were performed at thyssenkrupp Presta AG using an Instron 8802 uniaxial servo hydraulic fatigue testing machine. A sinusoidal load function with constant amplitude at a frequency of 4 Hz was used. A mechanical extensometer was used to measure strain and a FLUKE thermal imaging camera to monitor the surface temperature. For a temperature effect study, an environmental chamber with an electronic heating element was employed. Complete specimen separation was the failure criterion. If the dog bone did not break after 10E+6 cycles, the coupon was considered a runout. Runouts were excluded for the derivation of the SN curve equation. Load ratios were R = 0.1 and R = 0.5.

3. Experimental results

3.1 Micro-structure – Fiber orientation analysis

In Figure 2a and 2b the measured eigenvalues a_{11} of the fiber orientation tensor are plotted against the position through the specimen's thickness. Two different thicknesses for the core layer of the t = 3 mm (Fig. 2a) and t = 1.6 mm (Fig. 2b) samples were detectable. Approximately 0.8 mm for the 3 mm and 0.2 mm for the 1.6 mm specimens.

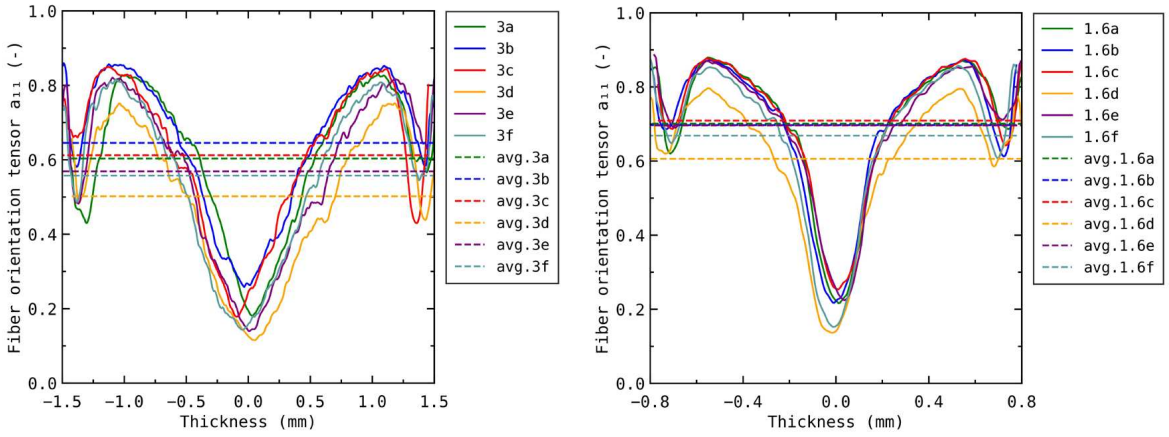

(a) *(b)*

Figure 2. Eigenvalue a_{11} in selected positions for plate thickness 3 (a) and 1.6 mm (b)

The µCT samples 3d, e and f have been extracted according to Figure 1b. A comparison of the average value 3a, 3b and 3c versus the µCT-measurements 3d, 3e and 3f showed a reduction of up to 23%. For the 1.6 mm specimens the delta lays around 13%. The average eigenvalues a_{11}

 ©2022 Francesco et al. doi:10.5075/epfl-298799_978-2-9701614-0-0 published under CC BY-NC 4.0 license

for the 1.6 mm specimen (a, b, c) milled out along the symmetry axis in flow direction were found to be constant. In all other cases a dependency of the extracted position was visible.

3.2 Quasi-Static material characterization

The stress-strain results from the quasi-static tests for two Fibre Orientation (FO) angles and two specimen thicknesses are shown in Figure 3. Strains at failure vary between 1.5 and 2.4%, depending on the FO angle. The test results are normalized by an arbitrary value for confidentiality reasons.

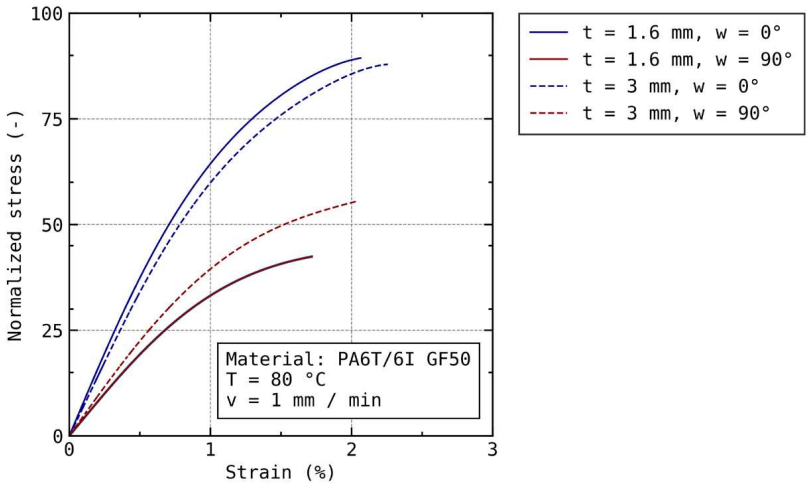

Figure 3. Comparison q. S. stress strain curves for 3 and 1.6 mm thick specimen at T = 80°C

3.3 Cyclic material characterization

Figure 4a and 4b present the fatigue test results as stress amplitude σ_a against the number of cycles to failure N_f in semi-logarithmic scale. All stress values have been normalized by an arbitrary value for confidential reasons.

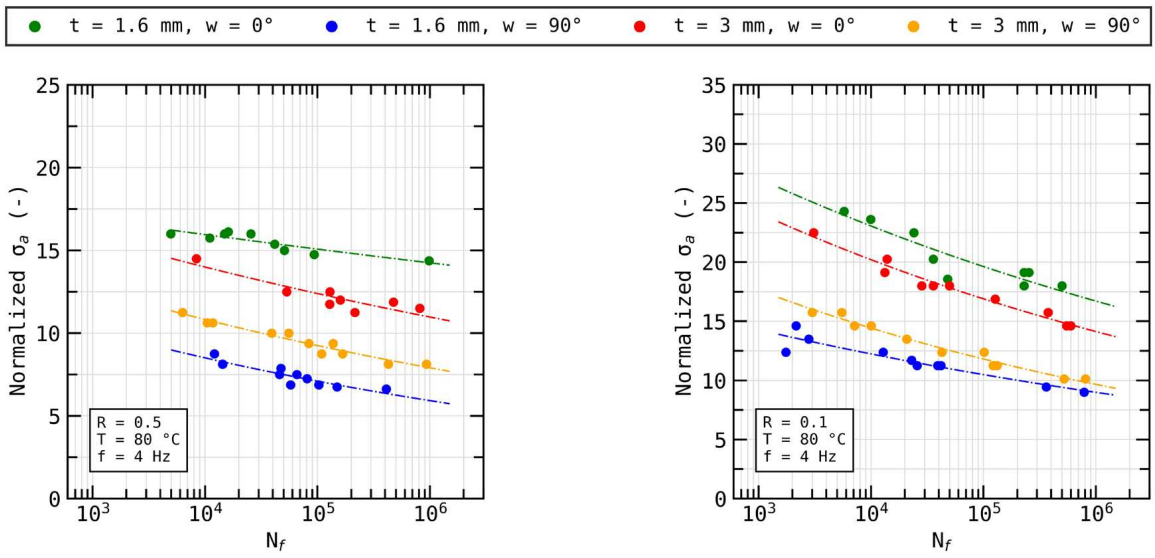

(a) *(b)*

Figure 4. Normalized S-N curves for 1.6 and 3 mm at R = 0.5 (a) 0.1 (b) for two orientations

 ©2022 Francesco et al. doi:10.5075/epfl-298799_978-2-9701614-0-0 published under CC BY-NC 4.0 license

Figures 5a and b display the quasi static and fatigue strength (residual strength at $N_f = 10^6$), normalized to the values at t = 1.6 mm thickness, as a function of specimen thickness. The quasi-static behavior is plotted for comparison purposes. The influence of the thickness on cyclic strength differs significantly from the correspondent influence on quasi-static strength, resulting in the conclusion that failure depends on the loading condition (static vs. cyclic). In regard to the R = 0.5 load ratio the normalized failure strength (extracted transversally, Figure 5b) drastically increases in comparison to the normalized failure strength of the coupon at R = 0.1 load ratio (extracted transversally, Figure 5a). The increase of around 24% leads to an approximation of the normalized failure strength in direction of the normalized quasi-static strength. For the longitudinal extracted specimens this trend cannot be confirmed. While quasi-static loading shows no significant difference in dependence of the thickness, the cyclic loading leads to a decrease of the fatigue strength. A higher decrease is detectable for R = 0.5.

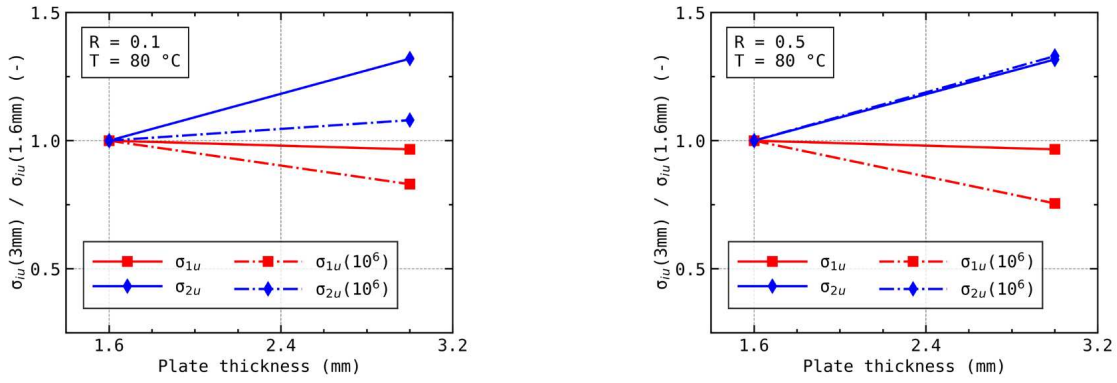

(a) *(b)*

Figure 5. Influence of thickness on normalized fatigue strength parameters for R = 0 (a) and R = 0.5 (b) compared to corresponding trends under quasi static loading

4. Fatigue criteria based one single set of parameters

In the present work the objective is to compare the ability of a strain and an energy-based criterion to predict fatigue failure. This criterion should be able to unify the fatigue data independently of the load ratio, fiber orientation, microstructure and specimen thickness using only one single set of parameters. Different criteria have been already proposed in [8-10]. Cyclic strain rate-based criteria showed good performance in regards to failure prediction. In this work, a comparison of the cyclic creep energy density and the cyclic creep strain rate is performed.

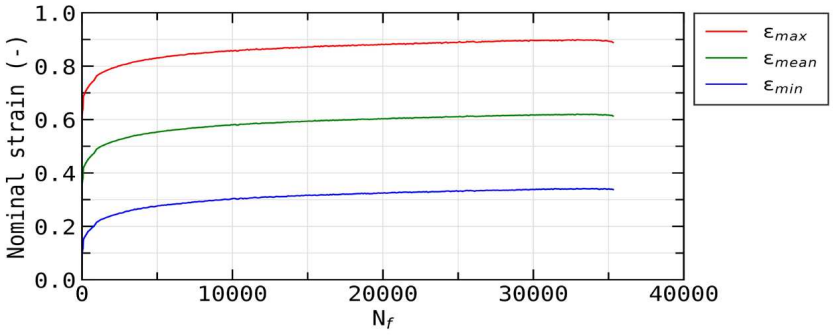

Figure 6. Trend of the maximal, minimal and mean strain until failure

 ©2022 Francesco et al. doi:10.5075/epfl-298799_978-2-9701614-0-0 published under CC BY-NC 4.0 license

Figure 6 depicts the trend of the minimum and maximum strain during fatigue testing of one of the tests performed on a longitudinally extracted 3 mm specimen, tested at R = 0.1. Based on these two values, the mean strain was also calculated. In this paper, the cyclic creep strain rate is calculated as the slope of the mean strain between 45% and 55% of the lifetime:

$$\dot{\varepsilon}_m = \frac{d\varepsilon_{mean}}{dN} \tag{1}$$

The calculated cyclic creep strain rate for the two analyzed thicknesses as well as the R-ratios was plotted as a function of cyclic to failure in Figure 7a.

The fatigue criterion allows to cluster the data independently of the thickness, fiber orientation and load ratio. The latter was possible since positive load ratios were considered within this investigation. The following power law criterion based on $\dot{\varepsilon}_m$ was identified:

$$\dot{\varepsilon}_m = aN_f^b \tag{2}$$

The Eq. (2) can be reformulated for the evaluation of the calculated lifetime as follows:

$$N_{f,calculate} = B(\dot{\varepsilon}_m)^p \tag{3}$$

The coefficients B and p are material dependent parameters.

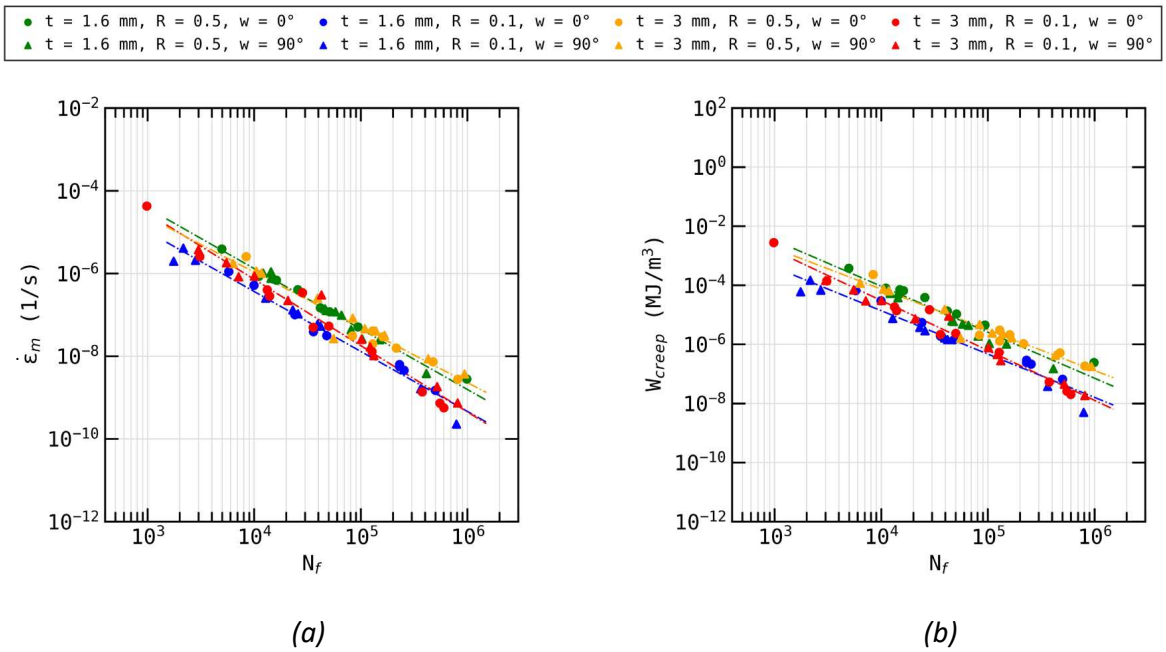

(a) *(b)*

Figure 7. Cyclic mean strain rate (a) and cyclic creep energy density (b) vs. number of cycles to failure for two load ratios, two specimen thicknesses and two orientations (dashed lines correspond to power-law fits, using one set of parameters for each R-Ratio, fiber orientation and specimen thickness).

The cyclic creep energy density (Fig. 7b) was determined by multiplying the cyclic mean strain rate $\dot{\varepsilon}_m$, between 45% and 55% of the lifetime, with the mean stress σ_{mean}. In this case, the cyclic creep energy density manages to group the two analyzed orientations and specimen thicknesses but fails to unify the results for different load ratios.

The following power-law criterion can be identified:

 ©2022 Francesco et al. doi:10.5075/epfl-298799_978-2-9701614-0-0 published under CC BY-NC 4.0 license

$$W_{creep} = aN_f^b \quad (5)$$

Eq. (5) can be rearranged for the evaluation of the lifetime such as:

$$N_{f,calculate} = B(W_{creep})^p \quad (6)$$

The coefficients B and p are material dependent parameters for the energy-based criterion.

The parameter set identification was carried out on the 0° fiber orientation specimen with a R-Value of 0.1 and a specimen thickness of t = 3 mm. To determine the criterion accuracy, the $N_{f,calculation}$ and $N_{f,experimental}$ are plotted on Fig. 8. The estimated lifetime $N_{f,calculation}$ is calculated by using Eq. (3) for the cyclic mean strain rate based criterion and Eq. (6) for the cyclic creep energy density. $N_{f,experimental}$ equals the experimental lifetime. For the cyclic mean strain rate based criterion, 76% of the calculated lifetime lays within scatter band two, whereas 98% was within scatter band three (Figure 8a). The calculated lifetime, compared with the one obtained experimentally, showed that the estimation of the cycles to failure by the cyclic mean strain rate based criterion can be used not only for the two R-Ratios and fiber orientations, but also for the wall thickness. For the cyclic creep energy based criterion, the usage of only one single set of parameters enables 71% of the fatigue lifetime data to be predicted by the criterion within a scatter band of a factor two. 90% of the predicted fatigue lifetimes are within a scatter band of factor three. The predictions were good for the analyzed load ratios.

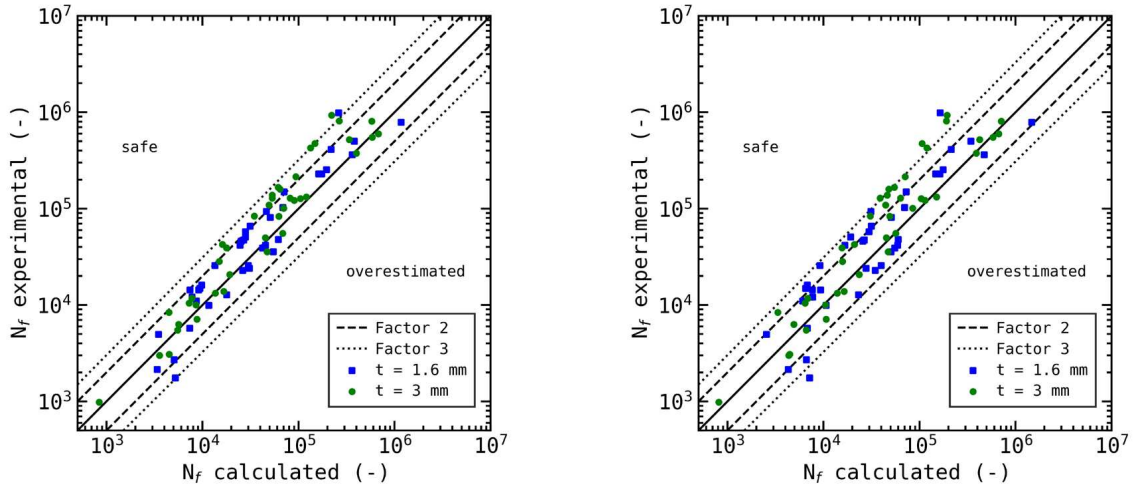

Figure 8. Fatigue criterion accuracy analysis based on one single set of parameters. (a) cyclic mean strain rate based and cyclic creep energy based criterion (b).

5. Conclusions

The present work analyzed the impact of the wall thickness onto the quasi-static and cyclic behavior. µCT scans were performed to evaluate the micro-structure as function of the thickness. The core layer thickness for the 3 mm specimens was approximately 0.8 mm and 0.2 mm for the 1.6 mm. In case of the 0° specimens, no significant static strength decrease could be detected in dependence of the wall thickness. The same did not apply for the 90° specimens, which showed an increase of the static strength with an increasing thickness of the probe. The 1.6 mm specimen always showed a higher fatigue strength compared to the 3 mm probe in case

 ©2022 Francesco et al. doi:10.5075/epfl-298799_978-2-9701614-0-0 published under CC BY-NC 4.0 license

of a longitudinal extraction to the main flow. An inverse behavior of the fatigue strength was witnessed, when analyzing the specimens which have been extracted transversally to the main flow direction. A strain-based and an energy-based criterion were chosen for the fatigue failure prediction using one single set of parameters. An independency of the thickness, fiber orientation and load ratio could be detected for the cyclic mean strain rate. The accuracy of the prediction lays between 76% (scatter band two) and 98% (scatter band three) in comparison to the experimentally determined lifetime. This research has been conducted by using only positive load ratios. To be able to evaluate a holistic material behavior with respect to the dependency of the wall thickness, an analysis including negative load ratios should be performed as well. Additionally, the conclusions drawn within this research should be tested and verified on a component or a system to understand if the procedure is still applicable for complex topologies. A final perspective could be to implement a cyclic mean strain rate numerical methodology in existing Finite Element tools.

6. References

1. Horst, J. J. (1997). Influence of fibre orientation on fatigue of short glassfibre reinforced Polyamide.
2. Bernasconi, A., Davoli, P., Basile, A., & Filippi, A. (2007). Effect of fibre orientation on the fatigue behaviour of a short glass fibre reinforced polyamide-6. International Journal of Fatigue, 29(2), 199-208.
3. De Monte, M., Moosbrugger, E., & Quaresimin, M. (2010). Influence of temperature and thickness on the off-axis behaviour of short glass fibre reinforced polyamide 6.6–cyclic loading. Composites Part A: Applied Science and Manufacturing, 41(10), 1368-1379.
4. Sauer, J. A., McMaster, A. D., & Morrow, D. R. (1976). Fatigue behavior of polystyrene and effect of mean stress. Journal of Macromolecular Science, Part B: Physics, 12(4), 535-562.
5. Sonsino, C. M., & Moosbrugger, E. (2008). Fatigue design of highly loaded short-glass-fibre reinforced polyamide parts in engine compartments. International Journal of Fatigue, 30(7), 1279-1288.
6. Bernasconi, A., & Kulin, R. M. (2009). Effect of frequency upon fatigue strength of a short glass fiber reinforced polyamide 6: a superposition method based on cyclic creep parameters. Polymer Composites, 30(2), 154-161.
7. Mallick, P. K., & Zhou, Y. (2004). Effect of mean stress on the stress-controlled fatigue of a short E-glass fiber reinforced polyamide-6, 6. International journal of fatigue, 26(9), 941-946.
8. Santharam, P., Marco, Y., Le Saux, V., Le Saux, M., Robert, G., Raoult, I., ... & Charrier, P. (2020). Fatigue criteria for short fiber-reinforced thermoplastic validated over various fiber orientations, load ratios and environmental conditions. International Journal of Fatigue, 135, 105574.
9. Raphael, I., Saintier, N., Rolland, H., Robert, G., & Laiarinandrasana, L. (2019). A mixed strain rate and energy based fatigue criterion for short fiber reinforced thermoplastics. International Journal of Fatigue, 127, 131-143.
10. Gillet, S., Jacopin, T., Joannès, S., Bedrici, N., & Laiarinandrasana, L. (2022). Short-term creep and low cycle fatigue unified criterion for a hybridised composite material. International Journal of Fatigue, 155, 106571.
11. Bernasconi, A., Cosmi, F., & Dreossi, D. (2008). Local anisotropy analysis of injection moulded fibre reinforced polymer composites. Composites Science and Technology, 68(12), 2574-2581.

 ©2022 Francesco et al. doi:10.5075/epfl-298799_978-2-9701614-0-0 published under CC BY-NC 4.0 license